

## Molecular Docking, Synthesis, Characterization and Antimicrobial Evaluation of 5-methyl thiazolidine-4-ones

Sarmad Saadi Hussein \*, Karima Fadhil Ali\*, and Fouad Abdulameer Al-Saady\*, Atheer Atiroğlu\*\*

\*Department of Pharmaceutical Chemistry, College of Pharmacy, Mustansiriyah University, Baghdad, Iraq.

\*\*Biomedical, Magnetic and Semiconductor Materials Application and Research Center, Sakarya University, Sakarya, Türkiye.

### Article Info:

Received June 2023

Revised July 2023

Accepted Aug 2023

Corresponding Author email:

[sarmad@bcms.edu.iq](mailto:sarmad@bcms.edu.iq)

Orcid: <https://orcid.org/0000-0002-5860-9869>

DOI : <https://doi.org/10.32947/ajps.v24i2.1033>

### Abstract:

To overcome the widespread emergence of drug resistant pathological agents, newer treatment options are required to be found urgently. This research aims to design new molecules with antimicrobial activities using computational methods and to synthesize these compounds.

The designed structures possessing thiazolidine-4-one heterocyclic moiety were evaluated for their *in vitro* antibacterial and antifungal activities and were found to exhibit antifungal and antibacterial properties. Molecular docking studies were conducted to examine the potential drug-protein interactions. Molecular characterization by spectral techniques (FT-IR,  $^{13}\text{C}$  NMR and  $^1\text{H}$  NMR) was carried out to confirm the identity of the synthesized compounds. The *in vivo* antimicrobial assays revealed that the compound F<sub>2</sub> contained the highest antifungal and antibacterial activity amongst the synthesized molecules.

**Keywords:** Antimicrobial, Antimicrobial resistance, Molecular docking, Thiazolidine-4-one

الإرساء الجزيئي والتخليق والتوصيف وتقييم مضادات الميكروبات لـ 5-مثيل ثيازوليدين-4-اون  
سرمد سعدي حسين\*, كريمة فاضل علي جواد\*, فؤاد عبد الامير ناجي\*, اثير عطراوغلو\*\*  
\*فرع الكيمياء الصيدلانية، كلية الصيدلة، الجامعة المستنصرية، بغداد، العراق.  
\*\*مركز أبحاث وتطبيقات المواد الطبية الحيوية والمغناطيسية وأشباه الموصلات، جامعة سقاريا، سقاريا، تركيا.

### الخلاصة:

إن إيجاد خيارات علاجية جديدة أمر ضروري للتغلب على مسببات الأمراض المقاومة للأدوية. يهدف هذا البحث لتصميم جزيئات كيميائية ذات خواص مضادة للبكتيريا باستخدام طرق حاسوبية ومن ثم تصنيع هذه المركبات مختبرياً. تم فحص الفعالية المضادة للميكروبات لهذه المركبات التي تحتوي على حلقة غير متجانسة ثيازوليدين-4-ون وتم إيجاد فعالية مضاد للبكتيريا والفطريات. تم عمل دراسة الإرساء الجزيئي لفحص الارتباطات المحتملة بين العقار والبروتين المستهدف. أجريت علمية التوصيف الطيفي للجزيئات من خلال تقنيات (FT-IR,  $^{13}\text{C}$  NMR and  $^1\text{H}$  NMR) للتأكد من هوية المركبات المصنعة.

**الكلمات المفتاحية:** مضادات الميكروبات، مقاومة البكتيريا، الإرساء الجزيئي، ثيازوليدين-4-اون

### Introduction

Antimicrobial Resistance (AMR) has been a long-standing problem facing clinicians ever since the first time these agents became

commercially available. After decades of continual use, now, all approved antibiotics have been documented to have resistance pathogens <sup>(1)</sup>. Moreover, the interest of



pharmaceutical companies to develop novel antibiotics have declined in recent years mainly due to lack of financial benefit from releasing of such new treatments <sup>(2)</sup>. To understand the calamity of the situation, it is estimated that annual deaths from drug-resistant pathogens could grow from 0.9 – 1.7 million death per year to 10 million deaths per year in 2050 <sup>(3)</sup>.

While the provision of new and novel antibiotics has greatly been neglected by big pharmaceutical companies, the academic scene has been testing various methods for drug discovery. Most notably, the recent advancement in machine learning and artificial intelligence have shown great interest and surge in utilization of such techniques for the development of new drug candidates <sup>(4)</sup>. The use of these in-silico methods to guide the process of drug discovery is well documented in literature. The information obtained from such method can supply the researcher with various abilities such as selection of the proper drug molecule to be synthesized from a small library, the potential drug pharmacokinetics, and the predicted binding affinity to its target <sup>(4,5)</sup>.

One method which incorporates deep machine learning (DML) techniques to be utilized in *de novo* drug design by which novel structure can be designed with desirable properties such as ease of synthesis, high validity and novelty. These methods depends of “feeding” the algorithm with data sets which allow it to generate diverse structures with the required properties <sup>(6)</sup>. Molecular docking, which is a method to test the binding affinity of a molecule to a certain receptor <sup>(7,8)</sup>. This tool has also had its share of machine learning involvement. This has enabled a chemical library with a size of billions of structures of molecules to be tested and docked to a certain binding site with reasonable time. This method incorporates machine learning by allowing

a small fraction of compounds of this library to be docked, the result of this process will be the learning data set for the algorithm. Which then will be able to predict the docking result of the entire library with fairly accurate results <sup>(9)</sup>. The thiazolidine-4-one moiety is a 5 membered ring heterocyclic structure which carries nitrogen, sulfur and a carbonyl group at position 4. The presence of these structural features made this scaffold a moiety with myriad action on a biological system. This has been utilized and many molecules containing this moiety were synthesized and evaluated for various pharmacological actions. Literature reports of this molecule serving various therapeutic utilities were reported such as anticancer <sup>(10)</sup>, antimicrobial <sup>(11,12)</sup>, antidiabetic <sup>(13)</sup>, antiparasitic <sup>(14)</sup>, anti-inflammatory <sup>(15)</sup>, antitubercular <sup>(16)</sup>, antiviral <sup>(17)</sup>, antioxidant <sup>(18)</sup>, anticonvulsant <sup>(19)</sup>, and analgesic activity <sup>(20,21)</sup>.

In this work, we synthesized four 5-methylthiazolidine-4-one derivatives which were previously checked to possess binding affinities with bacterial Penicillin-binding protein and with fungal (14a-demethylase) enzyme and evaluated their antibacterial and antifungal properties *in vitro*.

## Materials and Methods

### Materials

The starting materials p-Formyl phenyl boronic acid, p-Methoxybenzenesulfonyl hydrazide, 2,4,6-Trimethylbenzene sulfonyl hydrazide, p-toluenesulfonylhydrazide, Benzenesulfonylhydrazide, and 2-Mercaptopropionic acid were purchased from Sigma Aldrich (Germany).

### Equipment

Stuart melting point apparatus SMP30 (Germany) was used for uncorrected melting point measurement using capillary tube method. TLC silica gel in ethyl alcohol mobile phase were utilized to monitor the end of reaction. UV light lamp



was used for spot detection. IR and NMR analysis was carried out using Bruker VERTEX 70 FT-IR and Bruker Avance II 400 MHz NMR respectively. Magnetic stirrer was used during the reactions. Rotavapor® R-100 rotatory evaporator was utilized for removal of the solvent under reduced pressure.

### Molecular docking

Molecular docking studies were performed using The Cambridge Crystallographic Data Centre (CCDC) GOLD 2022 software. *Escherichia coli* Penicillin binding protein (PDB: 2ZC4) was used as the target for *in silico* binding affinity estimation. Ceftriaxone was used as a reference ligand by which our synthesized compounds were compared to. The candidal enzyme lanosterol demethylase (PDB: 5FSA) was used as the target for antifungal molecular docking study. The reference drug fluconazole was chosen as the ligand. All water molecules were found unnecessary and were removed. The original ligand of the enzyme was removed and set to be the binding region for our tested compounds. A total area of 10Å was chosen as binding pocket.

### ADMET studies

SWIS ADME free online tool was used for the purpose of predicting the pharmacokinetic properties of the synthesized molecules.

### Chemical Synthesis

The overall synthesis scheme is shown in (figure 1).

### Synthesis of sulfonyl hydrazone intermediates (I)

In a round bottom flask, a 5 mmol of p-formyl phenyl boronic acid was dissolved in ethyl alcohol, then a corresponding hydrazide was added to the mixture. Concentrated sulfuric acid was used as a catalyst. The flask was put on reflux for 3 hours. The completion was indicated by

appearance of a new spot in the TLC paper distinct than the starting material. The flask was left to cool in a refrigerator and was washed with distilled water and then left to dry <sup>(22)</sup>. The product was weighted and further characterized as below.

(I<sub>1</sub>) – IUPAC name: (4-((2-(phenylsulfonyl)hydrazinylidene) methyl) phenyl) boronic acid

Physical appearance: white powder. Yield: 89%. Melting point: 187 – 191 °C. FT-IR: 3348 cm<sup>-1</sup> (boronic acid hydroxyl), 3205 cm<sup>-1</sup> (NH of sulfonamide), 1610 cm<sup>-1</sup> (C=N of the imine), 1448 cm<sup>-1</sup> (Aromatic C=C), 1261cm<sup>-1</sup> (S=O sulfoxide of the sulfonamide).

(I<sub>2</sub>) – IUPAC name: (4-((2-((4-methoxyphenyl) sulfonyl) hydrazinylidene) methyl) phenyl) boronic acid

Physical Appearance: white powder. Yield: 85%. Melting point: 157-161 °C. FT-IR: 3439 cm<sup>-1</sup> (boronic acid hydroxyl), 2985 cm<sup>-1</sup> (CH<sub>3</sub> Asymmetric stretch), 3188 cm<sup>-1</sup> (NH of sulfonamide), 1600 cm<sup>-1</sup> (C=N of the imine), 1504 cm<sup>-1</sup> (Aromatic C=C), 1271cm<sup>-1</sup> (S=O sulfoxide of the sulfonamide).

(I<sub>3</sub>) – IUPAC name: (4-((2-tosylhydrazinylidene) methyl) phenyl) boronic acid

Physical appearance: white powder. Yield: 80%. Melting point: 143-146 °C. FT-IR: 3446 cm<sup>-1</sup> (boronic acid hydroxyl), 2924 cm<sup>-1</sup> (CH<sub>3</sub> Asymmetric stretch), 3200 cm<sup>-1</sup> (NH of sulfonamide), 1610 cm<sup>-1</sup> (C=N of the imine), 1512 cm<sup>-1</sup> (Aromatic C=C), 1309 cm<sup>-1</sup> (S=O sulfoxide of the sulfonamide).

(I<sub>4</sub>) – IUPAC name: (4-((2-(mesityl sulfonyl) hydrazinylidene) methyl) phenyl) boronic acid

Physical appearance: white powder. Yield: 90%. Melting point: 165-167 °C. FT-IR: 3553 cm<sup>-1</sup> (boronic acid hydroxyl), 2995 cm<sup>-1</sup> (CH<sub>3</sub> Asymmetric stretch), 3244 cm<sup>-1</sup> (NH of sulfonamide), 1606 cm<sup>-1</sup> (C=N of the imine), 1511 cm<sup>-1</sup> (Aromatic C=C),



1280  $\text{cm}^{-1}$  (S=O sulfoxide of the sulfonamide).

### Synthesis of 5-methyl thiazolidine-4-ones (F<sub>1-4</sub>)

A 3 mL of 2-mercaptopropionic acid was added to 1 mmol of the previously prepared sulfonyl hydrazones (I<sub>1-4</sub>). The mixture was placed in a magnetic stirrer and stirred for 3 hours at (60 °C). The mixture was allowed to cool and 5 mL of ethyl acetate was placed

in the mixture, then transferred to separatory funnel and the ethyl acetate upper layer was washed with 3 times with a fraction of 20 mL of sodium bicarbonate and additional amount of 10 mL distilled water. The water was removed from the ethyl acetate upper layer by treating it with anhydrous magnesium sulfate. A rotatory evaporator was utilized to remove solvent and allow the products (F<sub>1-4</sub>) to crystallize.<sup>(23)</sup>

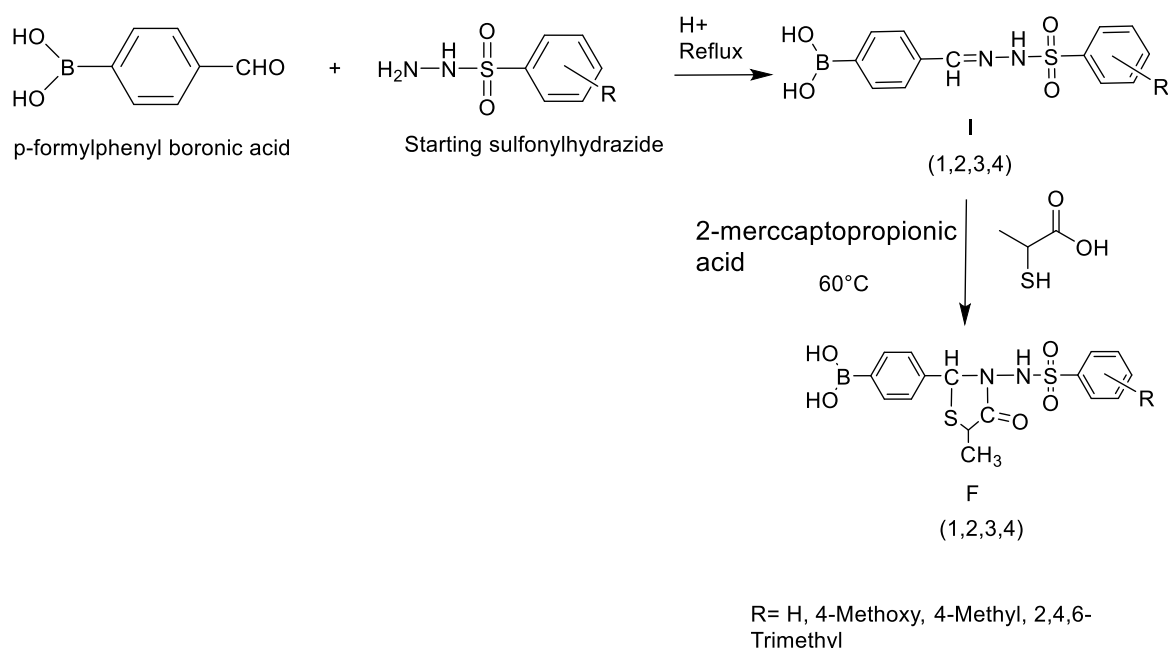


Figure 1. overall reaction scheme.

(F<sub>1</sub>) – IUPAC name - (4-(5-methyl-4-oxo-3-(phenylsulfonamido) thiazolidin-2-yl) phenyl) boronic acid

Obtained as white powder (61% yield), 129 – 132 °C. FT-IR: 3301  $\text{cm}^{-1}$  (O-H of boronic acid), 3206  $\text{cm}^{-1}$  (sulfonamide NH), 1729  $\text{cm}^{-1}$  (C=O of carbonyl), 1243  $\text{cm}^{-1}$  (C-N of amide), 1326  $\text{cm}^{-1}$  (S=O of sulfonamide). <sup>1</sup>H-NMR (Acetone-d<sub>6</sub>, 400 MHz),  $\delta$  (ppm): 1.25 – 1.26 (d, 3H, CHCH<sub>3</sub>), 3.93 (q, 1H, CHCH<sub>3</sub>), 5.93 (s, 1H, CH), 7.52 – 7.94 (m, 9H, ArH), 10.27 (s, 2H, B(OH)<sub>2</sub>), 11.58 (br s, 1H, NH). <sup>13</sup>C-NMR (Acetone-d<sub>6</sub>, 100

MHz),  $\delta$  (ppm): 19.26, 37.10, 61.45, 126.21, 127.64, 129.72, 133.53, 134.91, 135.42, 139.49, 147.73, 171.26.

(F<sub>2</sub>) – IUPAC name - (4-(3-((4-methoxyphenyl) sulfonamido)-5-methyl-4-oxothiazolidin-2-yl) phenyl) boronic acid

Obtained as white powder (69% yield), 162-166 °C. FT-IR: 3569  $\text{cm}^{-1}$  (O-H of boronic acid), 3330  $\text{cm}^{-1}$  (sulfonamide NH), 1729  $\text{cm}^{-1}$  (C=O of carbonyl), 1263  $\text{cm}^{-1}$  (C-N of amide), 1326  $\text{cm}^{-1}$  (S=O of sulfonamide). <sup>1</sup>H-NMR (Acetone-d<sub>6</sub>, 400



MHz),  $\delta$  (ppm): 1.32 – 1.34 (d, 3H, CHCH<sub>3</sub>), 3.12 (s, 3H, OCH<sub>3</sub>), 3.90 (q, 1H, CHCH<sub>3</sub>), 6.06 (s, 1H, CH), 7.29 – 8.00 (m, 8H, ArH), 8.98 (s, 2H, B(OH)<sub>2</sub>), 10.13 (br s, 1H, NH). <sup>13</sup>C-NMR (Acetone-d<sub>6</sub>, 100 MHz),  $\delta$  (ppm): 16.60, 35.34, 59.53, 62.91, 124.12, 124.87, 127.97, 128.34, 128.65, 132.51, 139.82, 145.15, 169.04.

(F<sub>3</sub>) – IUPAC name - (4-(5-methyl-3-((4-methylphenyl) sulfonamido)-4-

oxothiazolidin-2-yl) phenyl) boronic acid

Obtained as white powder (65% yield), 127

– 131 °C. FT-IR: 3511 cm<sup>-1</sup> (O-H of

boronic acid), 3312 cm<sup>-1</sup> (sulfonamide

NH), 1701 cm<sup>-1</sup> (C=O of carbonyl), 1262

cm<sup>-1</sup> (C-N of amide), 1344 cm<sup>-1</sup> (S=O of

sulfonamide). 1H-NMR (Acetone-d<sub>6</sub>, 400

MHz),  $\delta$  (ppm): 1.30 – 1.32 (d, 3H,

CHCH<sub>3</sub>), 2.42 (s, 3H, CH<sub>3</sub>), 3.87 (q, 1H,

CHCH<sub>3</sub>), 6.03 (s, 1H, CH), 7.24 – 7.87 (m,

8H, ArH), 8.99 (s, 2H, B(OH)<sub>2</sub>), 9.03 (br s,

1H, NH). <sup>13</sup>C-NMR (Acetone-d<sub>6</sub>, 100

MHz),  $\delta$  (ppm): 18.47, 19.79, 36.28, 60.54,

125.15, 127.09, 127.43, 128.56, 133.65,

135.73, 140.74, 143.56, 169.92.

(F<sub>4</sub>) – IUPAC name - (4-(5-methyl-4-oxo-3-((2,4,6-trimethylphenyl) sulfonamido)thiazolidin-2-yl) phenyl) boronic acid

Obtained off-white powder (55% yield),

139-143 °C. FT-IR: 3508 cm<sup>-1</sup> (O-H of

boronic acid), 3251 cm<sup>-1</sup> (sulfonamide NH),

1729 cm<sup>-1</sup> (C=O of carbonyl), 1273 cm<sup>-1</sup> (C-

N of amide), 1326 cm<sup>-1</sup> (S=O of

sulfonamide). (Acetone-d<sub>6</sub>, 400 MHz),  $\delta$

(ppm): 1.19 – 1.21 (d, 3H, CHCH<sub>3</sub>), 2.27 (s,

3H, ArCH<sub>3</sub>), 2.66 (s, 6H, (CH<sub>3</sub>)<sub>2</sub>), 3.86 (q,

1H, CHCH<sub>3</sub>), 7.04 – 7.80 (m, 6H, ArH),

10.49 (s, 2H, B(OH)<sub>2</sub>), 11.63 (br s, 1H,

NH). <sup>13</sup>C-NMR (Acetone-d<sub>6</sub>, 100 MHz),  $\delta$

(ppm): 19.16, 20.97, 23.22, 37.08, 61.49,

125.92, 131.69, 132.06, 132.10, 134.77,

134.86, 139.69, 145.80, 171.42.

## Antimicrobial activity

The synthesized molecules were evaluated for antimicrobial activity. *Klebsiella pneumonia* and *Escherichia coli* were used for gram negative antibacterial evaluation. *Staphylococcus epidermis* and *Staphylococcus aureus* were used for gram positive antibacterial evaluation. In all these cases, ceftriaxone was selected as a positive control. *Candida albicans* was selected for antifungal evaluation against which the activity of the synthesized molecules was compared to fluconazole as a positive control. Four consecutive dilutions were made to the compounds in order to obtain concentrations of (500, 250, 125, 62.5 µg/ml) which were introduced by a micropipette volume of 100 µL into the cultured species by well diffusion method. Then later the dishes were incubated at 37°C for 24 hours. The inhibition zones were recorded as diameter expressed in (mm).

## Results and Discussion

### FT-IR results

FT-IR characterization was made for both the intermediate (I<sub>1-4</sub>) and the final (F<sub>1-4</sub>) products. The first step of the reaction involved a nucleophilic attack by the sulfonyl hydrazide against the starting aldehyde to produce an imine bond. This bond was characteristic among all the 4 derivatives and was the standard to judge the success of the reaction by IR measurements at which this bond appeared in the range of 1600 to 1610 cm<sup>-1</sup> (Figure 2-5).





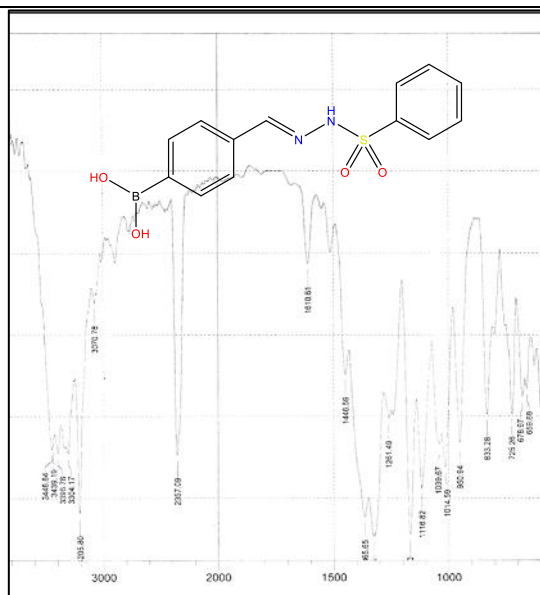


Figure 2. IR spectrum of I<sub>1</sub>

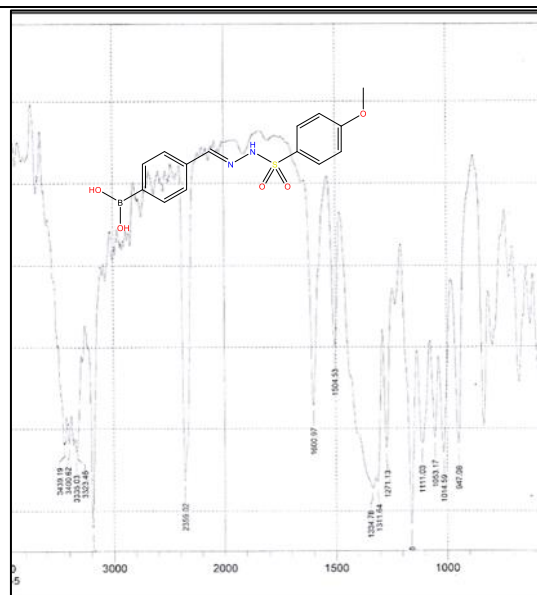


Figure 3. IR spectrum of I<sub>2</sub>

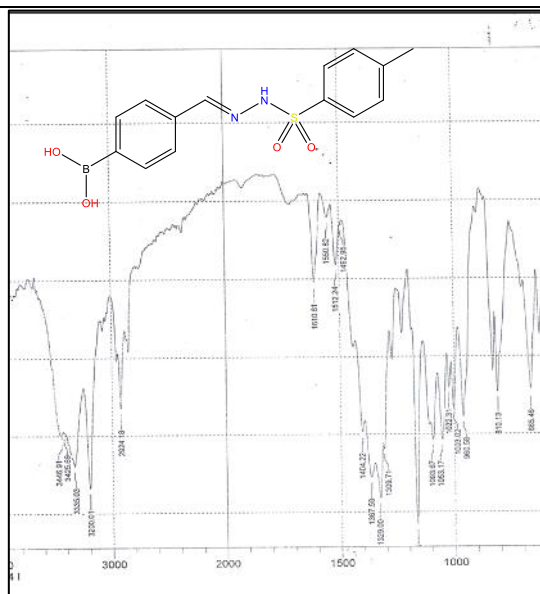


Figure 4. IR spectrum of I<sub>3</sub>

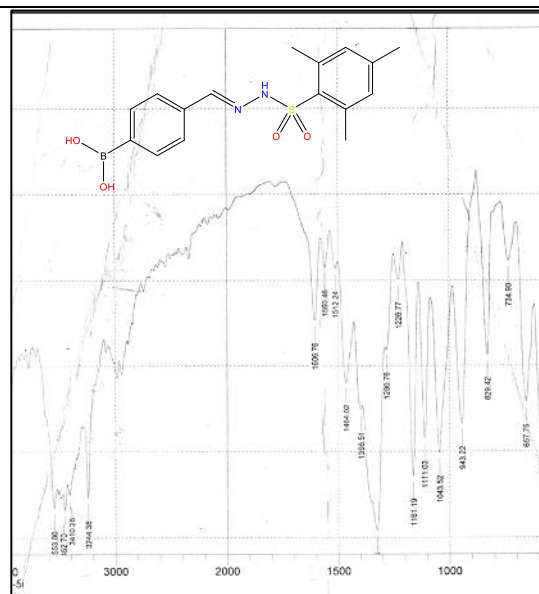


Figure 5. IR spectrum of I<sub>4</sub>

as for the IR of the final compounds, the ring closure with 2-mercaptopropionic acid produced the carbonyl bond which was

crucial for IR structure confirmation. This bond appeared in the range of 1701 – 1729  $\text{cm}^{-1}$  (Figure 6-9).

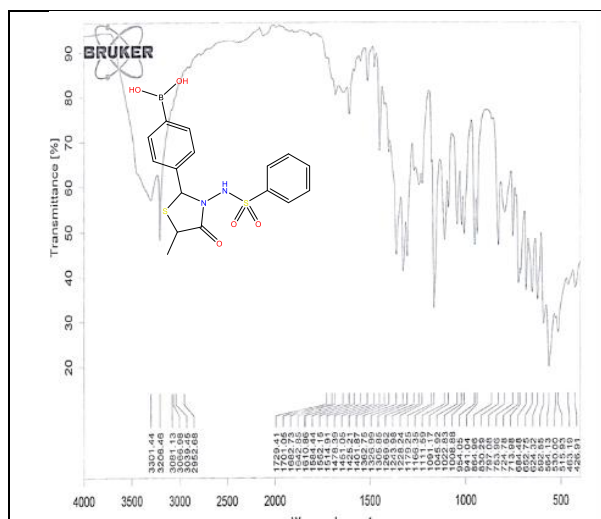


Figure 6. IR spectrum of F<sub>1</sub>

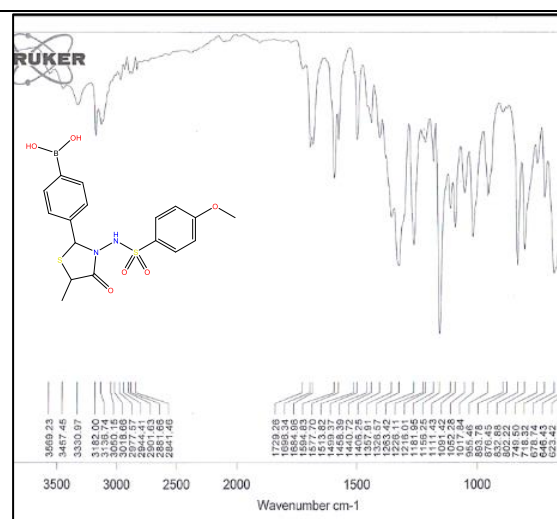


Figure 7. IR spectrum of F<sub>2</sub>

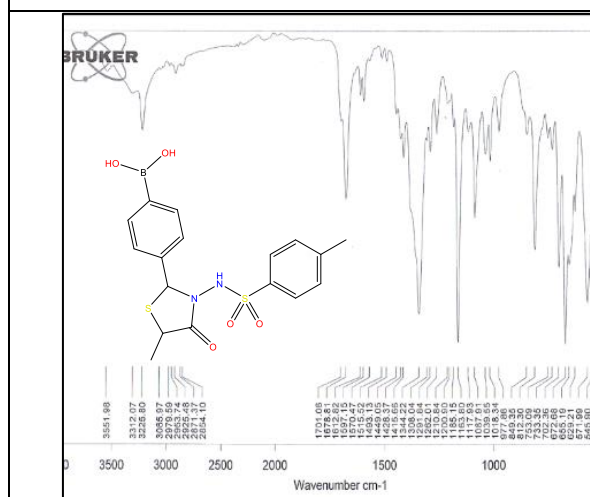


Figure 8. IR spectrum of F<sub>3</sub>

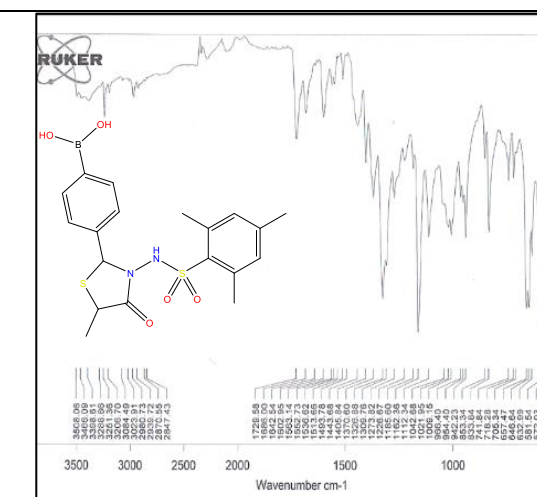


Figure 9. IR spectrum of F<sub>4</sub>

### <sup>1</sup>HNMR results

The final compounds were characterized with <sup>1</sup>HNMR in order to further confirm the identity of the final products (figure 9-12). Among the series of the prepared products, a trend can be seen for characteristic proton signals. The 5-methyl group of thiazolidine ring produced a doublet which were positioned in the shielded region of 1.19 to 1.34 ppm. The C5 carbon of the ring produced a quartet signal which were found in the region of 3.86 to 3.93 ppm. the sulfonamide NH

group produced a singlet at the region of 9.03 to 11.63 ppm. The two hydroxyl groups of boronic acid produced a singlet at the deshielded region of 8.98 to 10.49 ppm. The extreme deshielding of these protons can be explained by the fact that boron is a heavy metal atom with vacant orbital at which the lone pair of electrons of the oxygen can migrate into and produce resonance stabilized structures leading to a positive charge on the oxygen. This removes the local magnetic field that

normally shields the proton and cause it to resonate at higher chemical shift values (24).

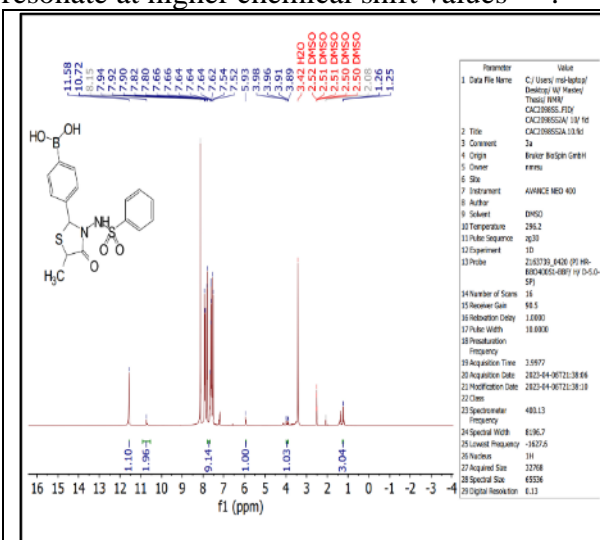


Figure 9.  $^1\text{H}$ NMR spectrum of F<sub>1</sub>

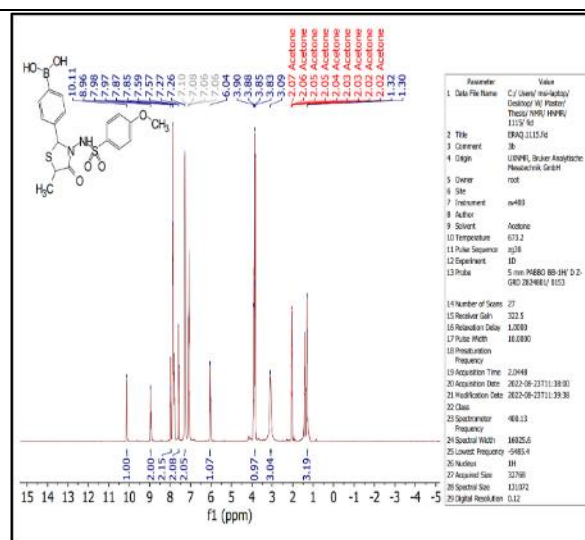


Figure 10.  $^1\text{H}$ NMR spectrum of F<sub>2</sub>

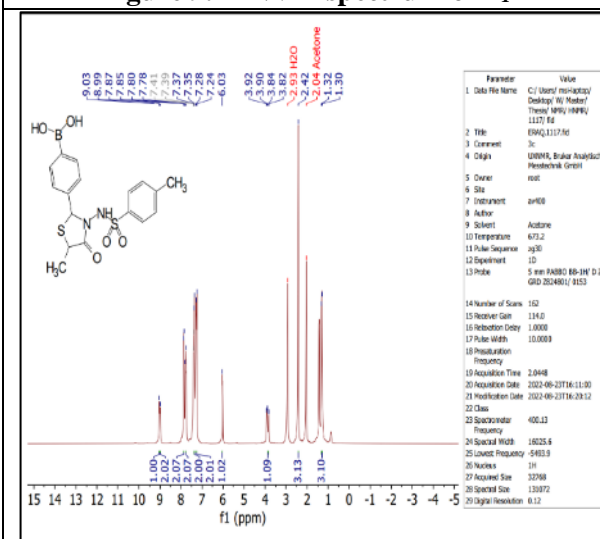


Figure 11.  $^1\text{H}$ NMR spectrum of F<sub>3</sub>

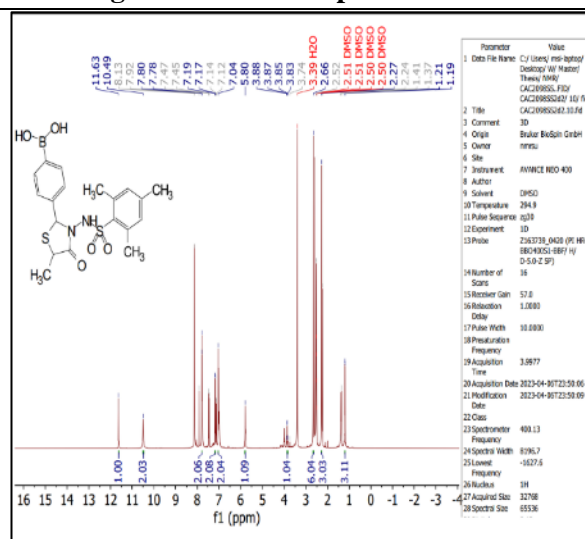


Figure 12.  $^1\text{H}$ NMR spectrum of F<sub>4</sub>

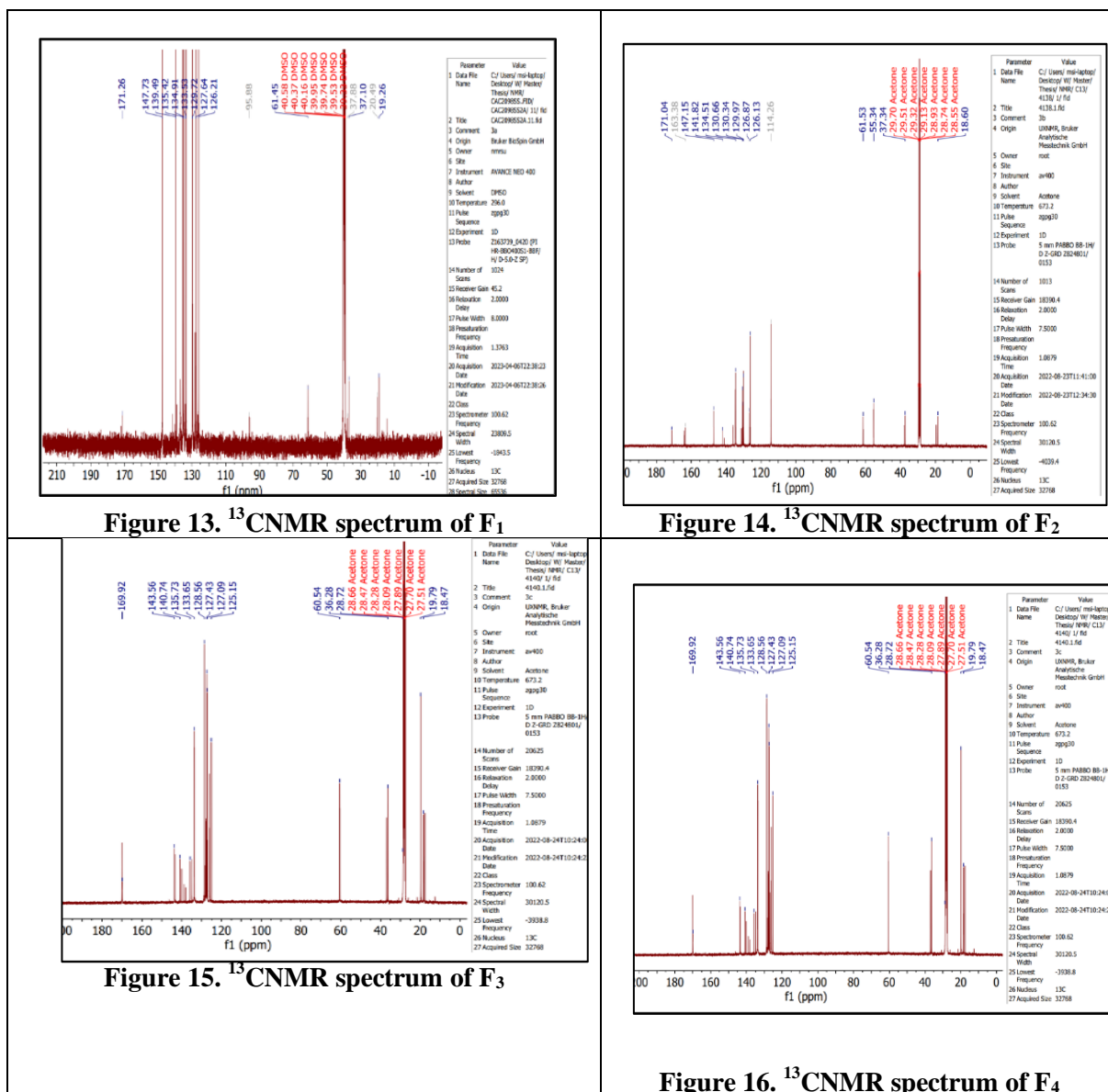
### $^{13}\text{C}$ NMR

$^{13}\text{C}$  NMR analyses were carried out to further reveal the carbon-hydrogen map of the compounds (Figure 13-16). The most

characteristic signal was the carbonyl group of the thiazolidine-4-one ring. This signal ranged between 169.04 to 171.42 ppm among the four derivatives.







### Molecular docking results

The obtained results were expressed as PLP fitness score, which is a scoring function employed by GOLD software to rank the ligands according to their fitness

to the receptor. The highest number being the most optimum fit. The results are expressed in table 1 and 2 for the bacterial and fungal targets respectively.

**Table (1): PLP fitness of the compounds *Escherichia coli* penicillin-binding protein (PDB: 2ZC4) in comparison to positive control drug (Ceftriaxone).**

Compound name	PLP Fitness Score	Interactions with amino acid residues
F <sub>1</sub>	70.8	Lys 340, Ser 395, Asn 397, Thr 550
F <sub>2</sub>	62.2	Ser 548, Ser 549
F <sub>3</sub>	75.6	Ser 337, Lys 340, Ser 395, Asn 397, Thr 550
F <sub>4</sub>	76.0	Ser 337, Lys 340, Ser 395, Asn 397, Thr 550



Ceftriaxone	66.4	Asn 397, Gly 459, Ser 571
-------------	------	---------------------------

**Table (2): PLP fitness of the compounds with *Candida albicans* protein 14-alpha demethylase (PDB: 5FSA) in comparison to positive control (Fluconazole).**

Compound name	PLP Fitness Score	Interactions with amino acid residues
F <sub>1</sub>	77.39	Tyr 132, Ser 378, Met 508
F <sub>2</sub>	77.33	Tyr 132, Ser 378
F <sub>3</sub>	85.86	Hem 580, Tyr 132, Ser 378, Met 508
F <sub>4</sub>	83.33	Tyr 132, Ser 378
Fluconazole	75.20	Hem 580

As can be seen, the interactions of the synthesized compounds differ completely from the reference drugs which can be attributed to difference in the basic pharmacophoric unit and the attached functional groups to it and therefore they tend to assume different pose and interact with different groups in the receptor site. For the interaction with the bacterial enzyme penicillin-binding protein (PBP), several hydrogen bonds between the

compounds and the enzyme residues stabilize the interaction and may contribute to biological activity. These proteins are responsible for imparting rigidity and keeping the integrity of the cell wall of the bacterial cell by promoting cross-linking of the peptidoglycan chains that protrude from the wall <sup>(25)</sup>. The figure 17 shows the interaction of the highest scoring compound F<sub>4</sub> with the residues of the target.

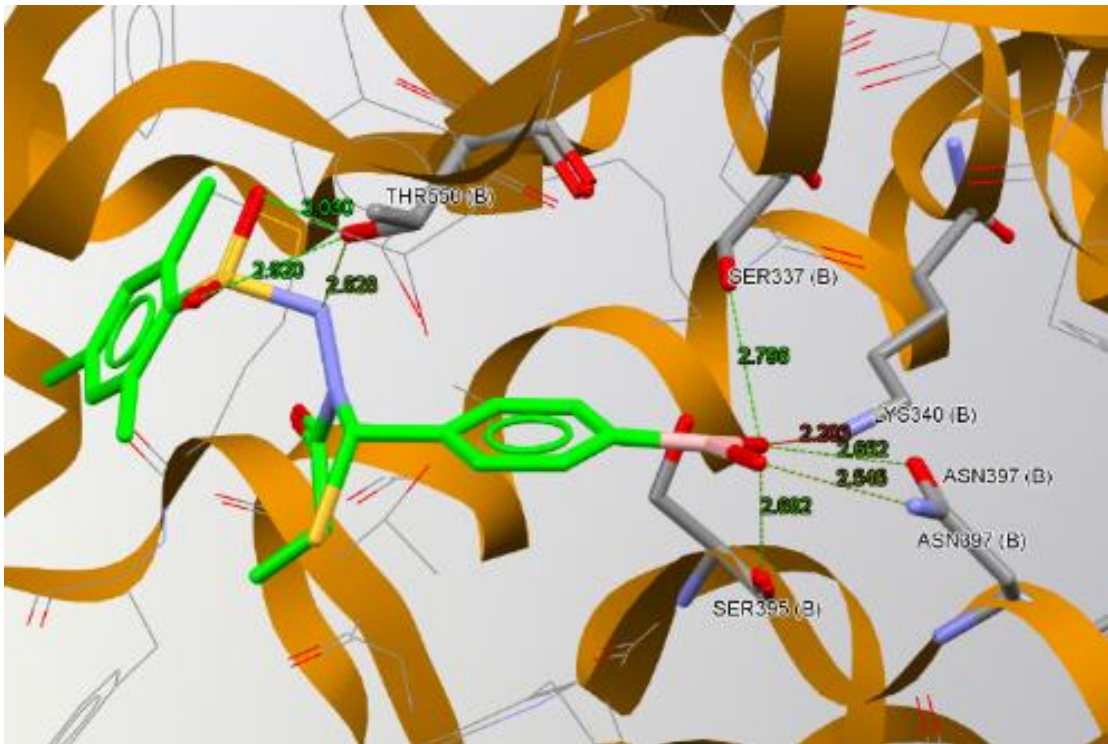


**Figure 17. Interaction of the highest scoring compound F<sub>4</sub> with the bacterial target penicillin binding protein of *E. coli*.**

The interaction with the candida enzyme 14- $\alpha$ -demethylase show both hydrogen bonding and metal-ligand coordination bonding. The heme portion of the enzyme contain a ferric group which binding to it is essential part of the antifungal activity. The reference drug fluconazole exerts its

activity by directly binding to the heme portion impeding the binding of the original substrate “lanosterol”<sup>(26)</sup>. The highest scoring derivative compound F<sub>3</sub> also show binding to the iron co-factor within the enzyme (figure 18).

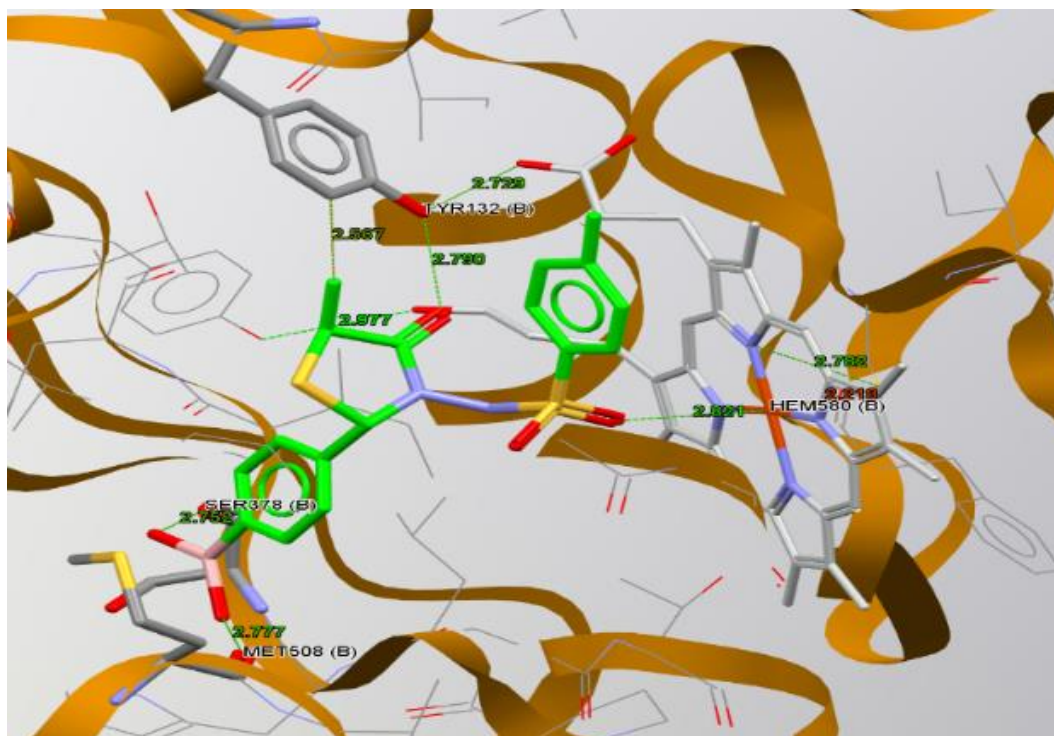


**Figure 18. Interaction of the highest scoring compound F<sub>3</sub> with the candidal protein 14- $\alpha$ -demethylase.**

### Antimicrobial Activity

The results for both antibacterial and antifungal activity are tabulated in table 3 and 4 respectively.

The chosen bacteria were among most clinical prevalent bacterial species. For instance, *Escherichia coli* is the most common infectious pathogen causing urinary tract infections (UTI)<sup>(27)</sup>. Similarly, *Klebsiella. Pneumonia* is the second most prevalent cause of UTI and it has also been implicated in respiratory tract infections<sup>(28)</sup>. The genus *Staphylococci* contains both *s. epidermis* and *s. aureus* which are among

the causative agents of minor to life threatening infections with rising antibiotic resistance<sup>(29)</sup>. The fungal species *candida albicans* are common invading pathogens involved in both superficial skin infections as well as mucus membrane candidiasis<sup>(30)</sup>. The overall results for antibacterial shows favorable activities for the synthesized compounds against gram-negative bacteria. While for gram-positive bacteria, the reference drug surpassed the tested compounds.

It can be seen from table 2 that the most active compound was F<sub>2</sub> especially at the

highest concentration where it exceeded all other derivatives. This compound is distinct from others by having a methoxy substituent group on the benzene ring which

may indicate an increase in activity can be seen when polar electron donating groups are substituted.

**Table 3: Antibacterial activity of the tested compound compared to the positive control drug ceftriaxone.**

Compound	Conc (µg/ml)	Inhibition zone (mm)			
		Gram Negative		Gram Positive	
		Klebsiella pneumonia	Escherichia coli	Staphylococcus epidermis	Staphylococcus aureus
Ceftriaxone	500	12	12	26	21
	250	11	12	25	19
	125	11	10	22	18
	62.5	-	-	19	17
F <sub>1</sub>	500	15	16	14	17
	250	13	15	13	15
	125	12	14	12	14
	62.5	11	13	11	13
F <sub>2</sub>	500	16	17	16	18
	250	13	15	13	17
	125	14	12	12	14
	62.5	13	12	10	12
F <sub>3</sub>	500	13	16	13	17
	250	12	14	13	14
	125	12	12	12	13
	62.5	11	11	11	12
F <sub>4</sub>	500	15	17	16	16
	250	14	16	15	15
	125	10	13	12	14
	62.5	10	-	12	13
DMSO	Pure	-	-	-	-

The antifungal effects of the tested compound showed a moderate activity indicated by the presence of inhibition zone. Compared to the reference drug

fluconazole, the activity was insignificant. Similar to antibacterial activity, compound F<sub>2</sub> achieved the highest effect among the prepared derivatives.

**Table (4): Antifungal activity of the tested compounds compared to the positive control drug fluconazole.**

Compound	Conc (µg/ml)	Inhibition zone of Candida albicans (mm)
Fluconazole	500	20
	250	18
	125	18
	62.5	17



F <sub>1</sub>	500	12
	250	12
	125	10
	62.5	10
F <sub>2</sub>	500	13
	250	11
	125	10
	62.5	10
F <sub>3</sub>	500	12
	250	12
	125	9
	62.5	-
F <sub>4</sub>	500	12
	250	12
	125	10
	62.5	-
DMSO	Pure	-

### ADMET properties

A preliminary ADMET properties of the synthesized molecules was obtained through SWISS ADME online prediction tool which provides a valuable information

regarding the possible *in vivo* pharmacokinetic properties in addition to other parameters such as drug-likeness and toxicity properties <sup>(26)</sup>.

**Table (5): Predicted physicochemical properties of the synthesized compounds.**

Compound	GI absorption	BBB penetration	Rotatable bonds	H-bond acceptors	H-bond donors	TPSA	Consensus Log P
F <sub>1</sub>	Yes	No	5	6	3	140.62	0.36
F <sub>2</sub>	No	No	6	7	3	149.85	0.32
F <sub>3</sub>	Yes	No	5	6	3	140.62	0.65
F <sub>4</sub>	Yes	No	5	6	3	140.62	1.22

\*TPSA: Topological polar surface area

As can be seen from the above table, all compounds possess possibility for oral absorption except the compound F<sub>2</sub> which may be explained due to the presence of a polar methoxy group which increased TPSA above the limit of possible oral absorption. However, the compounds still obeyed Lipinski rule for being a suitable oral drugs candidate as the number of rotatable bonds, molecular weight and number of hydrogen bond donors and acceptor was within the acceptable limit of this rule.

### Conclusion

The compounds were successfully synthesized, validated by spectroscopic techniques and were evaluated *in vitro* antimicrobial assays with good activities. This research prompts further testing to evaluate the actual *in vivo* effects and safety.

### References

- 1- Darby EM, Trampari E, Siasat P, Gaya MS, Alav I, Webber MA, et al. Molecular mechanisms of antibiotic





- resistance revisited. *Nat Rev Microbiol.* 2023;21(5):280–95.
- 2- Hegemann JD, Birkelbach J, Walesch S, Müller R. Current developments in antibiotic discovery. *EMBO Rep.* 2023;24(1).
- 3- Murray CJL, Ikuta KS, Sharara F, Swetschinski L, Robles Aguilar G, Gray A, et al. Global burden of bacterial antimicrobial resistance in 2019: a systematic analysis. *The Lancet.* 2022;399(10325):629–55.
- 4- Chen L, Yu L, Gao L. Potent antibiotic design via guided search from antibacterial activity evaluations. *Bioinformatics.* 2023;39(2).
- 5- Stoyanova R, Katzberger PM, Komissarov L, Khadhraoui A, Sach-Peltason L, Groebke Zbinden K, et al. Computational Predictions of Nonclinical Pharmacokinetics at the Drug Design Stage. *J Chem Inf Model.* 2023;63(2):442–58.
- 6- Wang M, Wang Z, Sun H, Wang J, Shen C, Weng G, et al. Deep learning approaches for de novo drug design: An overview. *Curr Opin Struct Biol.* 2022; 72:135–44.
- 7- Abdullah MT, Mahdi MF, Khan AK. Molecular docking, Synthesis and Characterization of New Indomethacin and Mefenamic Acid Analogues as Potential Anti-inflammatory Agents. *Al Mustansiriyah Journal of Pharmaceutical Sciences.* 2023;23(3):336–44.
- 8- Jameel BK, Raauf AMR, Abbas WAK. Synthesis, characterization, molecular docking, in silico ADME study, and in vitro cytotoxicity evaluation of new pyridine derivatives of nabumetone. *Al Mustansiriyah Journal of Pharmaceutical Sciences.* 2023;23(3):250–62.
- 9- Sivula T, Yetukuri L, Kalliokoski T, Käsänen H, Poso A, Pöhner I. Machine Learning-Boosted Docking Enables the Efficient Structure-Based Virtual Screening of Giga-Scale Enumerated Chemical Libraries. Cambridge; 2023.
- 10- Chawla A, Patial B, Sharma R, Akhter R, Sharma P, Kumar R. A Review on Anti-Cancer Activity of Benzopyrazole and Thiazolidine-4-One Nucleus. *International Journal for Research in Applied Sciences and Biotechnology.* 2022;9(3):166–74.
- 11- Desai NC, Shah KN, Dave BP, Khedkar VM. Design, Synthesis, Antimicrobial Activity and Molecular docking Studies of Pyridine Based Thiazolidine-4-one and Its 5-Arylidene Derivatives. *Analytical Chemistry Letters.* 2022;12(5):639–54.
- 12- Khalaf MH, Rasheed MK. Synthesis, identification and antimicrobial activity of thiazolidine-4-one and imidazolidine-4-one derived from 4,4-Methylenedianiline. *Int J Health Sci (Qassim).* 2022;6(S3):6425–37.
- 13- Ullah H, Uddin I, Rahim F, Khan F, Sobia, Taha M, et al. In vitro  $\alpha$ -glucosidase and  $\alpha$ -amylase inhibitory potential and molecular docking studies of benzohydrazide based imines and thiazolidine-4-one derivatives. *J Mol Struct.* 2022; 1251:132058.
- 14- Soni HI, Patel NB, Parmar RB, Chan-Bacab MJ, Rivera G. Microwave Irradiated Synthesis of Pyrimidine Containing, Thiazolidin-4- ones: Antimicrobial, Anti-Tuberculosis, Antimalarial and Anti-Protozoa Evaluation. *Lett Org Chem.* 2022;19(9):731–8.
- 15- Vasincu IM, Apotrosoaei M, Constantin S, Butnaru M, Vereștiuc L, Lupșoru CE, et al. New ibuprofen derivatives with thiazolidine-4-one scaffold with improved pharmaco-toxicological profile. *BMC Pharmacol Toxicol.* 2021;22(1):10.
- 16- Trotsko N. Antitubercular properties of thiazolidin-4-ones – A review. *Eur J Med Chem.* 2021; 215:113266.



- 17- İsaoglu M, Cesur N. Synthesis, Characterization and Antiviral Activities of Some Novel 4-Thiazolidinones Derived from Imidazo[2,1-b] [1,3] thiazole-5-carbohydrazone Hydrazones. *Anatolian Journal of Biology*. 2020; 1:22–30.
- 18- Dawood ZA, Khalid FD, Hameed AS. Synthesis, radical scavenging activity, antibacterial activity and molecular docking of a new thiazolidine-4-one and 1,3,4 oxadiazole derivatives of tolfenamic acid. *Teikyo Medical Journal*. 2022;45(2):5017–31.
- 19- Yamsani N, Sundararajan R. Design, In-Silico Studies, Synthesis, Characterization, and Anticonvulsant Activities of Novel Thiazolidin-4-One Substituted Thiazole Derivatives. *Biointerface Res Appl Chem*. 2022;13(4):366.
- 20- Sahiba N, Sethiya A, Soni J, Agarwal DK, Agarwal S. Saturated Five-Membered Thiazolidines and Their Derivatives: From Synthesis to Biological Applications. *Top Curr Chem*. 2020;378(2):34.
- 21- Mech D, Kurowska A, Trotsko N. The Bioactivity of Thiazolidin-4-Ones: A Short Review of the Most Recent Studies. *Int J Mol Sci*. 2021;22(21):11533.
- 22- Ismaeel S, Mahdi MF, Abdrazik BM. Design, Synthesis and Antibacterial Study of New Agents Having 4-Thiazolidinone Pharmacophore. *Egypt J Chem*. 2020;63(7):2592–603.
- 23- Mahdi MF, Rauf AMR, Kadhim FA. Design, Synthesis and Acute Anti-Inflammatory Evaluation of New Non-Steroidal Anti-Inflammatory Agents Having 4-Thiazolidinone Pharmacophore. *Journal of Natural Sciences Research*. 2015;5(6):21–8.
- 24- Hall DG. Structure, Properties, and Preparation of Boronic Acid Derivatives. Overview of Their Reactions and Applications. In: Hall DG, editor. *Boronic Acids: Preparation and Applications in Organic Synthesis and Medicine*. Wiley; 2005. p. 1–99.
- 25- Pazos M, Vollmer W. Regulation and function of class A Penicillin-binding proteins. *Curr Opin Microbiol*. 2021; 60:80–7.
- 26- Odiba AS, Durojaye OA, Ezeonu IM, Mgbeahuruike AC, Nwanguma BC. A New Variant of Mutational and Polymorphic Signatures in the ERG11 Gene of Fluconazole-Resistant *Candida albicans*. *Infect Drug Resist*. 2022; Volume 15:3111–33.
- 27- Ghaith Ahmed A, Mohammed Qasim Yahya MalAllah Al Atrakji, Wifaq M.Ali Alwattar. Antibacterial effect of ethyl acetate fraction of *Medicago Sativa* on *Escherichia Coli* in urinary tract infections. *J Fac Med Baghdad*. 2023;65(1):45–52.
- 28- Mohammed AM, Al-jobbery M jawed. Comparison between efficiency of propolis extracts and antibiotic treatment of *Klebsiella pneumonia* in rats. *Al-Qadisiyah Journal of Veterinary Medicine Sciences*. 2019;18(1):89–98.
- 29- Al-Taai HRR. Molecular Detection of *erm(A)*, *mef(A)* in *staphylococcus* spp and *streptococcus* spp Resistant to Macrolide from Different Clinical Infections. *Diyala Journal of Agricultural Sciences*. 2017; 9:1–15.
- 30- Mohammed MJ, Majid Mahdi F, Jassim HM. Formulation of Nystatin 2.4%, Neomycin Sulfate 0.35%, Dexamethasone 0.05% (w/w) Ointment. *Iraqi Journal of Industrial Research*. 2023;10(1):115–9.

